Pyrromethene Derivatives in Three-Component Photoinitiating Systems for Free Radical Photopolymerization

O. I. TARZI,[1,2] X. ALLONAS,[2] C. LEY,[2] J.-P. FOUASSIER[2]

[1]CIHIDECAR-CONICET, Department of Organic Chemistry, FCEyN-University of Buenos Aires, Pabellón 2—Ciudad Universitaria, (1428) Buenos Aires, Argentina

[2]Department of Photochemistry, UMR 7525 CNRS, Ecole Nationale Supérieure de Chimie de Mulhouse, Université de Haute-Alsace, 3 rue Alfred Werner, 68093 Mulhouse, France

Received 17 January 2010; accepted 24 March 2010
DOI: 10.1002/pola.24039
Published online in Wiley InterScience (www.interscience.wiley.com).

ABSTRACT: 1,3,5,7,8-pentamethyl pyrromethene difluoroborate complex (HMP) and 2,6-diethyl-8-phenyl-1,3,5,7-tetramethylpyrromethene difluoroborate complex (EPP) were used to initiate the polymerization of a diacrylate in a two- and a three-component photoinitiating system (PIS), together with an amine (ethyl-4-dimethylaminobenzoate, EDB) and triazine A (2-(4-methoxyphenyl)-4,6-bis(trichloromethyl)-1,3,5-triazine, TA) as coinitiators. For both pyrromethene dyes, the highest conversion was achieved with the three-component PIS. As these dyes have high-fluorescence quantum yields, steady state and time-resolved techniques were used to study the possible fluorescence quenching by the amine and the triazine, as well as laser flash photolysis to investigate the electron transfer process that occurs in these PIS from either the singlet or triplet excited states. The electron transfer reaction is evidenced by using time-resolved photoconductivity. Experiments show that the main interaction between the dye and both coinitiators is through its excited singlet state and the process is more efficient when TA is present. The beneficial effect noted when both coinitiators are used in a three-component system is ascribed to secondary reactions between the coinitiators and intermediates that lead to the generation of higher amount of initiating species and the recovery of the initial dye. © 2010 Wiley Periodicals, Inc. J Polym Sci Part A: Polym Chem 48: 2594–2603, 2010

KEYWORDS: electron transfer; kinetics; photochemistry; photopolymerization; pyrromethene dye; triazine

INTRODUCTION Visible light-induced photopolymerization has emerged as an attractive technology for the polymer formation in a wide variety of applications. For example, laser direct imaging, graphics arts, holography, and dental materials require irradiation in the visible spectrum to benefit from laser technologies or simply to avoid UV damaging effects on skin.[1,2] Some dyes absorbing in the visible region have been reported to be photoreducible in the presence of amines.[3,4] These compounds belong to the families of xanthenes, fluorones, acridines, phenazines, thiazenes, and so on. For example, methylene blue is well known to react from its triplet state with amine to initiate the photopolymerization of acrylates. The photoreduction is accompanied with an important photobleaching of the dye, rendering the photopolymerization of thick samples possible under visible light. The photobleaching is not so important in the case of xanthenes or fluorones, although the polymerization can be very efficient. Very good efficiencies were reported using thionine, rose bengal, eosin Y, erythrosin, riboflavin as photoinitiators, and coinitiators, such as amines, sulfinates, carboxylates.[3–5] In the case of amine as coinitiator, the reaction involves a hydrogen abstraction from the amine to form the semireduced form of the dye. These systems are able to shift the spectral sensitivity of photopolymers up to the red region of the visible spectrum. However, dye/coinitiators systems were not developed significantly in the industry. Very often, dark reactions take place that lead to poor shelf life of the formulation, an effect that was detrimental to their industrial use for a long time. In addition the conversion of the monomer to polymer was generally limited. Indeed, for most of the industrial applications, conversion of more than 60% have to be reached, a goal that is difficult to achieve with conventional dye/coinitiator photoinitiating systems (PIS).

Certain additives improve the polymerization efficiency, leading to the development of the so-called three-component PIS.[6–14] The mechanism involved is usually rather complex and is based on chemical secondary reactions. It was reported that different radical intermediates generated during the irradiation and in the subsequent polymerization reaction react with the additive to give new reactive radicals.

Pyrromethene dyes (Py) were first synthesized at the end of the 80's by Boyer and coworkers.[15,16] As it is known, these dyes present intense absorption and fluorescence bands in

Correspondence to: X. Allonas (E-mail: xavier.allonas@uha.fr)

the green-red visible region of the electromagnetic spectrum and exhibit high fluorescence quantum yields.[17,18,42–44] The best known application of these dyes is in the laser field, where they showed higher laser efficiency than rhodamine dyes.[19] This led to an important number of articles related to the study of the photophysics and photostability of the existing Py in different media, such as solution, solid matrices, polymers, nanocomposites, and so on, as well as its correlation with laser properties.[20–22] The knowledge of the properties of existing Py led to the synthesis of new compounds of this family that may optimize the laser action.[23,24] Besides their use as laser dyes, Py have also shown very good performance as sensitizing dyes in free radical photopolymerization, with the idea of using the photopolymers in industrial applications, such as photoimaging, holography, computer-to-plate, and so on. They have been used as photoinitiator with an acrylate to produce a holographic recording material,[25] as sensitizer dye with a benzophenone derivative as a radical generating reagent,[26] as photoinitiator together with a photoacid generator.[27] In relation to this last application, Py have been previously studied in our laboratory as an example of an application to printing technology, in which they interact by a sensitization mechanism with a photoacid generator to produce a positive working photopolymer.[28,29] This article reports the use of Py as part of a three-component PIS for radical polymerization in the visible region of the spectrum, together with an amine and a triazine as coinitiators. Triazines have been used in the field of photopolymerization as photoinitiators, and also as coinitiators in PIS, reacting in that case through an electron transfer mechanism together with an electron donor.[11,30–33] In this study, we examined the ability of the systems formed by Py/amine, Py/triazine, and Py/amine/triazine, to initiate polymerization under visible light. To understand their efficiency in terms of monomer conversion, the photochemistry of these systems was investigated by means of steady state and time resolved spectroscopies.

EXPERIMENTAL

Py derivatives EPP and HMP were gift from Dr. S. Suzuki and Prof. Takahara from the Chiba University. They were synthesized as described in literature.[34,35] 2-(4-methoxyphenyl)-4,6-bis(trichloromethyl)-1,3,5-triazine (TA) was provided by PCAS company (Produits Chimiques Auxiliaires et de Synthèses, Longjumeau, France) and ethyl-4-dimethylaminobenzoate (EDB) was purchased from Aldrich (Scheme 1). The monomer used was an ethoxylated bisphenol A diacrylate (EBPOA, SR 349, gift from Sartomer) with a viscosity of $\eta = 1600$ mPa s at 25 °C. UV-grade acetonitrile was purchased from Fluka. All reactants were used as received without further purification.

The polymerization experiments were carried out by the real-time FTIR technique using a Vertex 70 FTIR spectrometer (Bruker Optik), equipped with MIR and NIR light sources, and a MCT detector working in the rapid scan mode, allowing an average of 4 scans/s collection rate (4 cm^{-1} resolution). The IR spectra are then recorded during the 15 min of

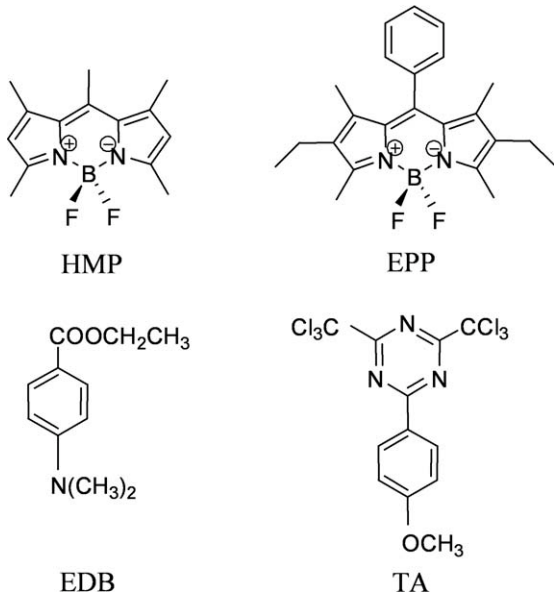

SCHEME 1 Compounds used in this study.

irradiation using a Xenon arc lamp (Hamamatsu L8253, 200 W), which was adapted to the FTIR spectrometer by means of a light guide. A longpass filter, absorbing wavelengths below 395 nm, was used to avoid direct irradiation of the monomer or TA by UV light. To prevent the diffusion of oxygen into the sample under exposure, laminate experiments were carried out, placing the resin between two polypropylene films and two BaF_2 crystal windows. The thickness of the sample was adjusted using a 50 μm teflon spacer. The spectra were recorded between 600 and 3900 cm^{-1}. The kinetics of the polymerization were measured by following the disappearance of the C=C bond stretching signal at 1637 cm^{-1}. The initial absorbance of the sample at 1637 cm^{-1} was adjusted around 1.

The degree of conversion, directly related to the decrease in IR absorbance A_{1637}, was calculated as:

$$\text{Conversion}(\%) = \frac{(A_{1637})_0 - (A_{1637})_t}{(A_{1637})_0} \times 100 \qquad (1)$$

where $(A_{1637})_0$ and $(A_{1637})_t$ are the area of the IR absorption peak at 1637 cm^{-1} of the sample before exposure and at a given irradiation time t, respectively. Keeping in mind that there is no real linear portion of the conversion versus time curves, a good estimate of the maximum rate of polymerization R_p was determined as the slope of these conversion profiles as $R_p/[M]_0$ at the inflection point, $[M]_0$ being the initial concentration of the monomer.[36] The composition of each formulation is shown in Table 1.

Ground state absorption and fluorescence spectra were recorded on a Beckman DU640 spectrophotometer and a Horiba Jobin Yvon FluoroMax 2 spectrofluorometer, respectively. Fluorescence lifetimes were measured using a pulsed

TABLE 1 Weight Composition of the Samples, Corresponding EDB/TA Molar Ratio, Final Conversion Obtained After 15 min of Irradiation, Maximum Polymerization Rate $R_p/[M]_0$ and Inhibition Time

Run	Dye (%)	EDB (%)	TA (%)	Molar Ratio EDB/TA	Inhibition Time (s)	$R_p/([M]_0 \times 100)$ (s^{-1})	Final Conversion (%)
EPP 1	0.1	2.5	–	–	n.m.[a]	0.05	28.6
EPP 2	0.1	–	1	–	10.7	0.9	42.1
EPP 3	0.1	2.5	1	5/1	8.4	1.2	50.3
EPP 4	0.1	1.1	2.3	1/1	4.0	2.2	56.6
EPP 5	0.1	0.4	5.5	1/5	2.4	5.1	74.1
HMP 1	0.1	2.5	–	–	n.m.[a]	0.04	18.2
HMP 2	0.1	–	1	–	15.1	0.51	29.3
HMP 3	0.1	2.5	1	5/1	6.3	1.4	58.6
HMP 4	0.1	1.1	2.3	1/1	4.0	1.1	50.1
HMP 5	0.1	0.4	5.5	1/5	1.5	6.0	76.5

[a] n.m.: not measurable.

laser diode emitting at 372 nm and a TCSPC FluoroMax-4 spectrofluorometer (Horiba Jobin Ybon). Quenching rate constants k_q were determined from Stern–Volmer plots of reciprocal values of fluorescence intensity or the lifetime of the triplet state versus the quencher concentration.

Steady-state photolysis experiments were performed using a 200 W Hg lamp (Oriel Instruments, Newport) with a cut-off filter at 395 nm. Acetonitrile solutions were placed on 3 mL stoppered quartz cells and irradiated during 2 h. The reactions were monitored by UV–vis absorption spectroscopy.

Laser flash photolysis experiments (LFP) were carried out in a 1 cm cell, exciting at 355 nm (HMP) and 532 nm (EPP) with a nanosecond Nd-YAG laser (Powerlite 9010, Continuum), operating at 10 Hz. The transient absorption analysis system (LP900, Edinburgh Instruments) uses a 450-W-pulsed Xe arc lamp, a Czerny-Turner monochromator, a fast photomultiplier, and a transient digitizer (TDS 340, Tektronix).[37] The instrumental response is about 7 ns. The observation wavelength is indicated in each case. Experiments were performed in acetonitrile under Ar bubbling.

The redox potentials were measured by cyclic voltammetry using a potentiostat (Princeton Applied Research 263A) at a scan rate of 1 V/s in acetonitrile, as described elsewhere.[28]

Time resolved photoconductivity allows the study of ions generated by actinic light in solution. Two rectangular (8×10 mm^2) platinum plates, separated by a distance $d = 8$ mm, are placed inside a rectangular quartz cell. A high continuous voltage of about 300–500 V is applied between the two electrodes during the experiment. The solution is irradiated by the same nanosecond pulsed laser beam used for LFP experiments, which is collimated between the two platinum plates. The transient photocurrent $i(t)$ arising by the generation of ions in the solution is measured through a resistance R_c. The resulting voltage $[U(t) = R_c \times i(t)]$ is then monitored by a Tektronix DSA 601 transient digitizer. The measured potential $U(t)$ is then proportional to the number of photogenerated ions $n(t)$, the amplitude of the electrical field E (and then to the applied high-voltage as $E = U/d$), the ions mobility and to the resistance R_c.[38,39] This latter could be adjusted between 50 Ω to some kΩ to detect very small photocurrents.

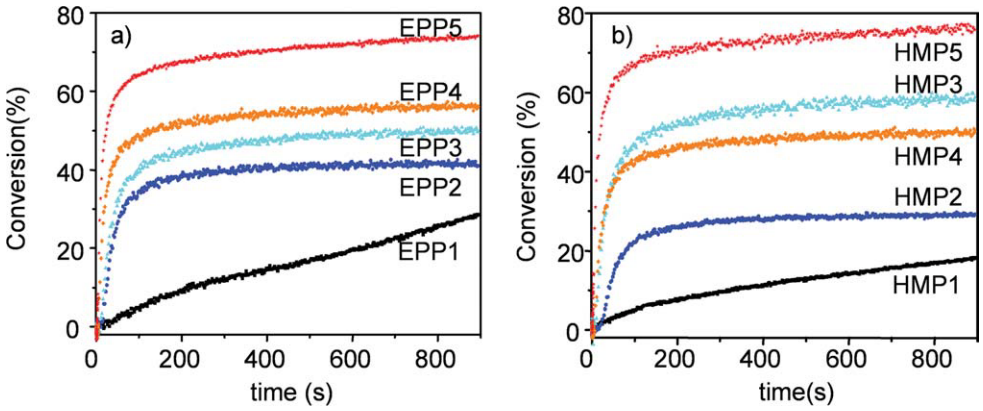

FIGURE 1 Comparative study of the photopolymerization of EBPDA using different photoinitiating systems based on the two Py dyes: EPP and HMP. [Color figure can be viewed in the online issue, which is available at www.interscience.wiley.com.]

TABLE 2 Photophysical and Electrochemical Properties of HMP and EPP (from [17])

	HMP	EPP
λ_{max} (nm)	492	521
ε_{max} (mol^{-1} dm^3 cm^{-1})	95,100	72,000
E_S (kJ/mol)	240	226
ϕ_f	0.93	0.77
τ_0^S (ns)	6.0	5.8
E_T (kJ/mol)	–	157
τ_0^T (μs)	–	39
E_{ox} (V/SCE)	1.21	1.10
E_{red} (V/SCE)	−1.18	−1.16

Maximum absorption wavelength λ_{max}, molar extinction coefficient ε_{max}, singlet state energy E_S, fluorescence quantum yield ϕ_f, singlet state lifetime τ_0^S, triplet state energy E_T and corresponding lifetime τ_0^T, half-wave oxidation and reduction potentials E_{ox} and E_{red}, respectively.

RESULTS AND DISCUSSION

Polymerization Experiments

The efficiency of different combinations of Py, EDB, and TA as PIS for the polymerization of acrylates, was evaluated using the real-time FTIR technique. The different formulations, in weight percentages of each component, for each dye are detailed in Table 1. No significant photopolymerization was detected in the absence of dye. Figure 1 shows the corresponding kinetics observed for EPP (a) and HMP (b), and Table 1 shows the final conversions, polymerization rates and inhibition times for all runs after 15 min of irradiation. As expected, the behavior is strongly dependent on the composition of the PIS. Both EPP and HMP dyes exhibit similar behavior that depends mostly on the nature of the coinitiator. The use of amine in the Py/EDB system leads to a poor and slow conversion of the monomer. This is quite surprising, as amines are known as highly efficient coinitiator when a hydrogen abstraction favors the formation of aminoalkyl radicals.

On the contrary, the system Py/TA exhibits a good reactivity with both higher rate of polymerization and final conversion. However, the best results were obtained for the three-component system Py/EDB/TA: the addition of TA to the Py/EDB system increased the polymerization rate as well as the final conversion of the acrylate compared with the two-component systems. More interestingly, a clear beneficial effect is found in that case, and it can be seen that the performance is directly related to the molar concentration of TA present in the formulation. Increasing the proportion of TA also increases the polymerization rate and decreases the inhibition time, suggesting that the presence of TA is crucial to achieve a high-conversion of the monomer. From the comparison of Runs 3 and 5, an excess of TA with respect to EDB is necessary to obtain the best results.

UV–Vis absorption spectra of the formulations 1–3 of both dyes were recorded before and after RT FTIR experiments. The decrease in absorbance is more important for the system containing TA in agreement with the most important efficiency of the TA containing systems with respect to the EDB based ones. Steady state photolysis performed in acetonitrile solutions of Py/EDB, Py/TA, and Py/EDB/TA in the same weight ratios as in the RT-FTIR formulations showed that TA increases the photobleaching of both dyes more than EDB, in agreement with the results observed in photopolymerization experiments.

Excited state Reactivity

Singlet and Triplet State Reactivity

As both EPP and HMP exhibit high-fluorescence quantum yields (Table 2), the fluorescence quenching by TA and EDB was first studied. For both dyes, quenching rate constants k_q^S of the singlet excited state of the dyes with EDB and TA were determined in acetonitrile (Table 3), showing values close to the diffusion rate constant ($k_d = 2 \times 10^{10}$ M^{-1} s^{-1}).

LFP experiments were carried out on EPP in acetonitrile solution, exciting at 532 nm. The detection of ^{3}EPP was made at 440 nm.[28] The values of the triplet state quenching rate constants k_q^T show that the EPP triplet state quenching by EDB and TA is less efficient than the quenching of its singlet excited state (Table 3). However, the lifetime of ^{3}EPP being higher than the singlet state one, one can expect a significant contribution of the triplet state quenching in the formation of initiating species.

After laser excitation of HMP alone, a second-order decay is observed at 400 nm, which is practically unaffected by oxygen. This decay corresponds to the overlap of both the absorption of the dye triplet state ^{3}HMP and its radical cation $HMP^{\bullet+}$. The latter is also observed at 420 nm without

TABLE 3 Fluorescence k_q^S and Triplet State k_q^T Quenching Data and Gibbs Free Energy ΔG_{et} Changes for HMP and EPP with EDB and TA in Acetonitrile

	k_q^S (M^{-1} s^{-1}); ΔG_{et} (eV)		k_q^T (M^{-1} s^{-1}); ΔG_{et} (eV)	
Dye	EDB	TA	EDB	TA
HMP	1.3×10^{10}; −0.24	5.4×10^9; −0.16	6.6×10^9	n.m.[a,b]
EPP	7.0×10^9; −0.11	1.7×10^{10}; −0.12	8.0×10^6; +0.60	2.0×10^6; +0.59

[a] n.m.: not measurable.
[b] not calculable.

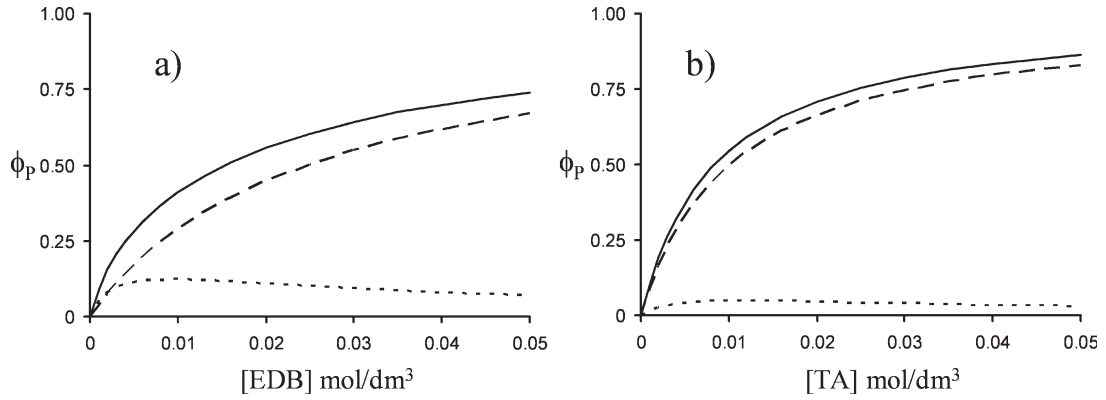

FIGURE 2 Calculated quantum yield of product formation ϕ_P from EPP quenching of singlet excited state (dashed line), triplet state (dot line) and addition of both routes (plain line) in the case of (a) EDB and (b) TA as quenchers.

superposition of other transient species. Observation of the triplet state at 400 nm allows the determination of the triplet state quenching rate constant by EDB which is found close to the diffusion limit, in sharp contrast to the EPP behavior. However, it can be anticipated from the high-fluorescence quantum yield of HMP (Table 2) that the triplet state quantum yield ϕ_T^{HMP} is lower than 0.07. Therefore, the triplet state will not yield to an important formation of reactive species from HMP.

Because of the redox properties of the dyes (Table 2) and the coinitiators, the mechanism for the quenching of EPP and HMP excited states likely involves an electron transfer process. The values of the Gibbs free energy change for the photoinduced electron transfer ΔG_{et} from one excited state is given by the Rehm Weller equation[40]:

$$\Delta G_{et} = E_{ox} - E_{red} - E^* + C \quad (2)$$

where E_{ox} and E_{red} are the half-wave oxidation and reduction potentials for the donor (EDB; $E_{ox} = 1.07$ V/SCE) and the acceptor (TA; $E_{red} = -1.12$ V/SCE), respectively, and E^* is the energy of the excited state. The coulombic term C is usually neglected in polar solvent. As can be seen in Table 3, the calculated values for the intermolecular singlet electron transfer reactions are favorable, indicating that both dyes can be reduced in the presence of the electron donor EDB or oxidized with TA.

The triplet energy level of HMP is not known. Consequently, ΔG_{et} values from ^{3}HMP were not calculable. However, as stated above, the low quantum yield of ^{3}HMP prevent any significant contribution of the triplet state reactivity. In the case of ^{3}EPP, it can be seen from Table 3 that this triplet state reaction is not thermodynamically favorable, in line with the low values of rate constants.

From these results, one can conclude that the dyes react with the coinitiators EDB or TA from both the singlet and the triplet states in the case of EPP, and mainly through the quenching of the first excited singlet state for HMP. The reaction proceeds through the formation of a geminate radical ion pair, which can recombine through a back electron transfer process or separate into free ions. The latter process explains the formation of the radical anion of the dye when EDB is used as quencher, or the radical cation of the dye when TA is used instead.

Radical Ion Quantum Yield

Whatever the reaction route (singlet vs. triplet) for EPP, the same transient radical ion is expected. Therefore, the maximum whole yield of radical ion ϕ_P will depend on the quenching rate constants of both the singlet and the triplet states and on the quencher concentration $[Q]$ according to:

$$\phi_P = \left(1 - \frac{1}{1 + k_q^S \tau_0^S [Q]}\right) + \left(\frac{\phi_T}{1 + k_q^S \tau_0^S [Q]}\right)\left(1 - \frac{1}{1 + k_q^T \tau_0^T [Q]}\right) \quad (3)$$

where τ_0^S and τ_0^T are the lifetime of the singlet and the triplet states, respectively, in the absence of quencher. ϕ_T is the triplet quantum yield in the absence of quencher. No information about EPP triplet quantum yield is available. However, the fluorescence quantum yield being 0.77, a maximum value of $\phi_T = 0.23$ can be assumed.

Figure 2 shows the calculated evolution of ϕ_P from both the singlet and triplet states in acetonitrile. It can be seen that the triplet state contribution is much more effective in the case of EDB than TA. However, at high-degree of singlet state quenching, the contribution of the triplet route decreases, as a consequence of the decreasing formation of the triplet state.

Reactivity of the Radical Ions

From the transient spectra reported previously,[28] the ground state photobleaching of EPP under addition of EDB can be observed at 520 nm. Accordingly, it can be seen in Figure 3(a) that the ground state depletion increases with increasing concentration of EDB, as a consequence of the formation of the dye radical anion EPP$^{\bullet -}$. Unfortunately, the latter species can not be observed under our experimental conditions. The initiating radicals in this case could come mainly from

the EDB radical cation, after the loss of proton to generate the aminoalkyl radical $EDB^{\bullet}_{-H}$It should be noted that this reaction will compete with the back electron transfer from $EPP^{\bullet-}$ to $EDB^{\bullet+}$ within the ion pair, as well with the recombination of the free ions. The effect of both these reactions can be observed in the increasing transient absorption in Figure 3(a) showing a recovery of the EPP ground state after about 100 μs. More details can be obtained from photoconductivity experiments. In that case, the system studied is irradiated in solution between two platinum plates that are connected to a high-voltage supply. Therefore, the photogenesis of free ions is detected as a transient current. It should be noted that irradiation of EPP alone doesn't lead to significant photocurrent. It can be seen in Figure 3(b) in the presence of EDB, the generation of the photocurrent proceeds in two steps: (i) a fast rise occurring within the laser pulse, which is attributed to a photoinduced electron transfer reaction between the EPP singlet excited state and EDB and (ii) a slow growth for which the rate of appearance is in agreement with the triplet state decay at this concentration of EDB: the rate constant is measured as 0.018 μs^{-1} from the rising photocurrent, in line with the pseudo first-order rate constant of 0.032 μs^{-1} that can be calculated from the triplet quenching rate constant k_q and [EDB] ($k_q \times [EDB] = 8\ 10^{-6} \times 0.004 = 0.032\ \mu s^{-1}$). Therefore, the formation of ions is clearly demonstrated. Moreover, the signal ratio between the slow and fast rises is measured as 0.77, in qualitative agreement with a value of 1.00 that can be derived from eq 3 at the concentration of 4×10^{-3} M for EDB. It should be noted that the photocurrent doesn't decay within the time window of 500 μs, a fact that could be attributed to the deprotonation process of $EDB^{\bullet+}$.

As stated above, when HMP is used with EDB as coinitiator the triplet state is quenched with a value close to the diffusion rate constant, not observing an increase in the signal of the radical cation $HMP^{\bullet+}$: as EDB amine acts as an electron donor, the electron transfer reaction of HMP excited states and EDB leads to $HMP^{\bullet-}$ and $EDB^{\bullet+}$ (cf. Scheme 2). Monitoring the ground state photobleaching at 492 nm leads to the observation of a decreasing absorbance of the dye, in line with the results obtained for EPP. This demonstrates that the reaction between HMP-excited states and EDB behave similarly to that of EPP. From all these results, the low conversion observed in the photopolymerisation for the EPP/EDB PIS could be explained by a low quantum yield of radical formation from $EDB^{\bullet+}$.

For the system EPP/TA, the photobleaching of the ground state increases with increasing the concentration of TA, as shown in Figure 4. This indicates that the photochemical reaction between EPP-excited states and TA yields to the formation of transient species. This ground-state bleaching is also more significant than with EDB, in agreement to what was observed in steady-state photolysis. According to the electron transfer reaction, the radical cation $EPP^{\bullet+}$ is easily detected at 400 nm.[29] It can be seen from Figure 5(a) that $EPP^{\bullet+}$ is formed within the laser pulse, as a consequence of its formation mainly from the singlet state of the dye to TA. Again in this case, the interaction between EPP and TA occurs mainly through the excited singlet state of the dye, although a part of triplet reaction can not be ruled out. This leads to the corresponding radical cation of EPP and the radical anion of TA. The latter species afterwards loses chloride anion to give the initiating radical $TA^{\bullet}_{-Cl}$, as was demonstrated for other triazine derivatives in presence of phenothiazine.[41] Interestingly, the recorded cyclic voltammogram for TA in acetonitrile exhibits an irreversible reduction wave at -1.12 V/SCE and a noticeable oxidation wave at 1.01 V/SCE indicating a cleavage process within the radical anion $TA^{\bullet-}$. It is expected that the chloride anion is expelled in a fast time scale, preventing the $EPP^{\bullet+}/TA^{\bullet-}$ system to undergo a back electron transfer process. This contention is also confirmed by the photocurrent profile [Fig. 5(b)], which doesn't decay within the time window. This is typical for the formation of long-lived ion such as Cl^-. Similarly to the system EPP/EDB, the signal rise exhibits both a fast and a slow components that are respectively, ascribed to the reaction from the singlet state and the triplet state. Moreover, the ratio of the triplet route over the singlet one is of the same order of magnitude as the calculated one from eq 3: 0.28 and 0.09, respectively. This set of reaction explains the high-reactivity of the EPP/TA system compared with the EPP/EDB one.

HMP exhibits toward TA a similar reactivity than EPP: at 400 nm it is possible to observe an increase of $HMP^{\bullet+}$ signal, which clearly evidences the electron transfer process from HMP to TA.

Turning now to the study of the three-component system, transient absorption spectroscopy at 400 nm shows that the signal of $EPP^{\bullet+}$ formed from the interaction EPP/TA (with excess of TA with respect to EDB) decreases under addition of EDB (Fig. 6). This indicates that the amine reacts with the radical cation of EPP formed from the interaction of EPP excited states with TA [Fig. 6(a)]. At the same time, the photobleaching of EPP ground state is lowered when EDB is added to the EPP/TA system [Fig. 6(b)]. This means that the reaction of EDB with $EPP^{\bullet+}$ leads to the recovery of the dye ground state. The reaction is expected to proceed through an electron transfer process from EDB to $EPP^{\bullet+}$. From the value of the oxidation potential of EPP, the reduction potential of $EPP^{\bullet+}$ is assumed to be $+1.10$ V/SCE. Therefore, the free energy of the electron transfer reaction between EBD and $EPP^{\bullet+}$ is estimated to be -0.03 eV, a value that would lead to a fast rate constant of interaction [Scheme 2(a)]. In the case of HMP, the corresponding ΔG_{et} value between $HMP^{\bullet+}$ and EDB is -0.14 eV, showing that the reaction is also thermodynamically favorable.

Similarly, if the deactivation of the excited state of the dye proceed through a photoinduced electron transfer with EDB [Scheme 2(b)], the radical anion of the dye is formed. The latter can react with TA leading to the recovery of the dye ground state. In this case, one can assume that the oxidation potential of $EPP^{\bullet-}$ and $HMP^{\bullet-}$ are -1.16 V/SCE and -1.18 V/SCE, respectively. This leads to the calculation of ΔG_{et}

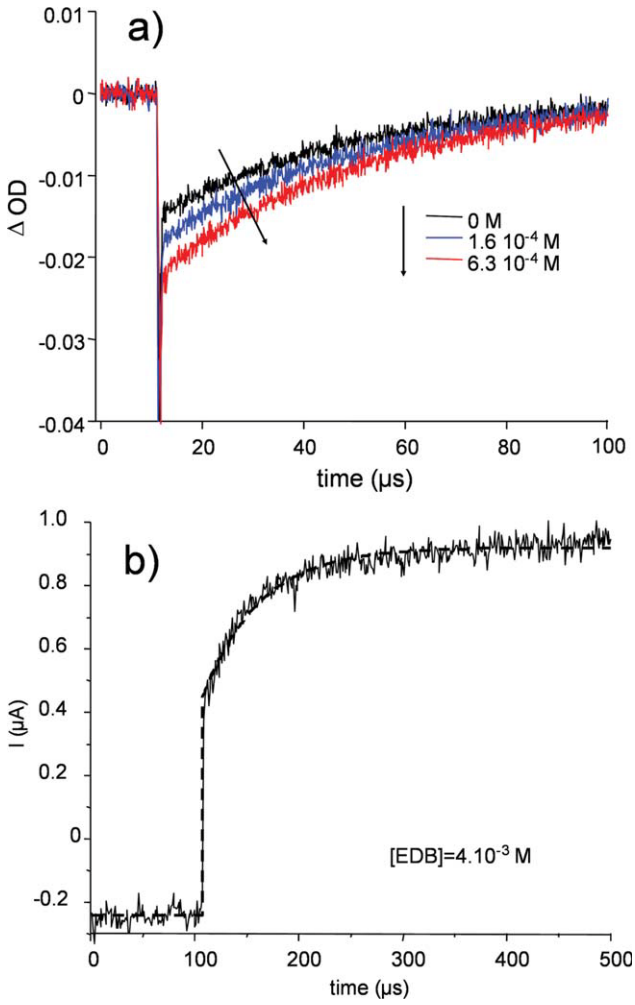

FIGURE 3 (a) Transient absorption recorded at 520 nm of an argon saturated solution of EPP with various concentrations of EDB and (b) photocurrent signal at [EDB] = 4×10^{-3} M with the corresponding best fit. [Color figure can be viewed in the online issue, which is available at www.interscience.wiley.com.]

values of −0.04 and −0.06 eV for EPP and HMP, respectively, showing that this reaction is exergonic enough to be operative.

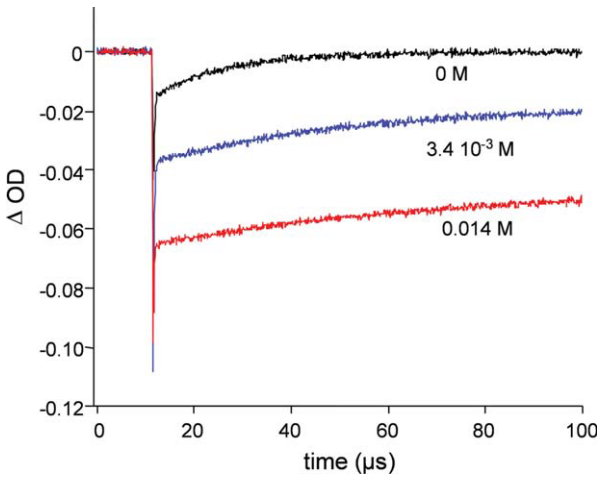

FIGURE 4 Transient absorption recorded at 520 nm of an argon saturated solution of EPP with various concentrations of TA. [Color figure can be viewed in the online issue, which is available at www.interscience.wiley.com.]

Photoinitiation Efficiency

From all these experiments, it turns out that the photoreactions from the excited states of the Py dyes are very efficient with both TA and EDB. These photoreactions lead to the formation of initiating species, and therefore, to the conversion of the monomer. In a viscous medium, the quenching rate constants can be limited by the diffusion process. A rough estimate of the diffusion rate constant can be given by:

$$k_d = \frac{8R_T}{3\eta} \tag{4}$$

This leads to the value of $k_d = 4.1 \times 10^6$ M^{-1} s^{-1} for the monomer used. Consequently, the quantum efficiency of the Py excited state deactivation by a given quencher Q will depend on $k_d \times [Q]$ for most of the photoreactions reported in Table 3. Therefore, the relative efficiency of the corresponding photochemical processes will be mainly dependent on the concentration of the coinitiators.

In the case of the Runs 3 (EPP 3 and HMP 3), the highest concentration of EDB makes the excited states quenched by

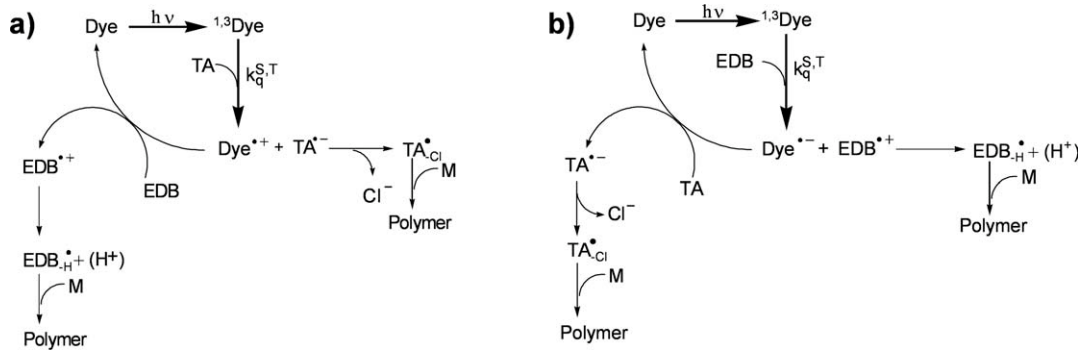

SCHEME 2 Mechanisms of reaction of three-component photoinitiating systems based on Py, EDB and TA.

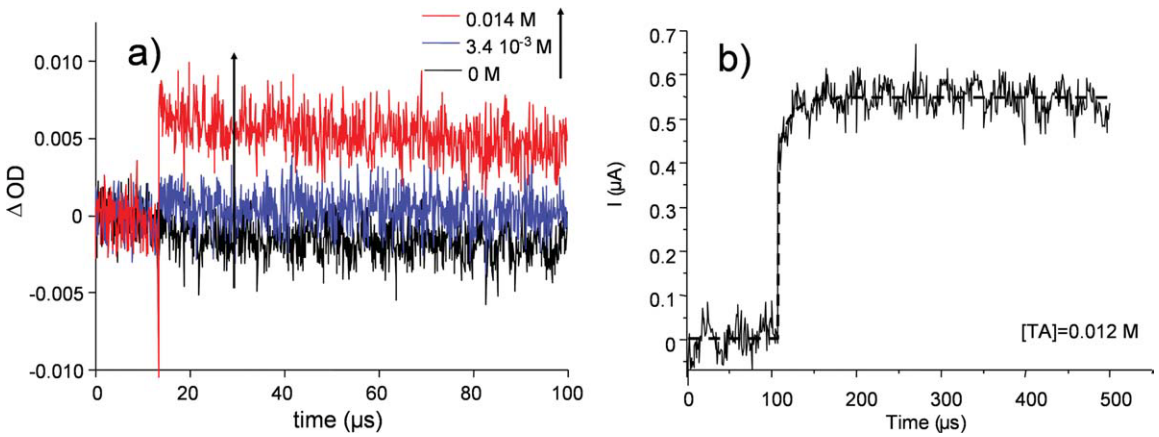

FIGURE 5 (a) Kinetic traces recorded at 400 nm of an argon saturated solution of EPP at different concentrations of TA and (b) photocurrent signal at [TA] = 0.12 M with the corresponding best fit.

EDB, leading to some initiating radical (after a deprotonation process) and the radical anion $Py^{\bullet -}$. This latter is able to react with TA leading to the recovery of the Py ground state and additional initiating species [Scheme 2(b)]. The fact that Runs 3 has higher efficiencies than Runs 1 is in good agreement with the expected reaction of TA with the dye radical anion [Scheme 2(b)]. The combination of coinitiators EDB and TA have clearly a beneficial effect on the photopolymerization process.

By contrast, in the case of Runs 5 (EPP 5 and HMP 5), the deactivation of the Py excited states will be mainly governed by the photoreaction with TA, which is at higher concentration than EDB. This leads to the formation of initiating radicals and a radical cation $Py^{\bullet +}$. The lifetime of this latter is long enough to react with EDB, giving rise to the recovery of the initial dye and a new initiating species [Scheme 2(a)].

Finally, as the cleavage of $TA^{\bullet -}$ is expected to be more efficient than the deprotonation of $EDB^{\bullet +}$, it is not surprising that Runs 5 lead to more efficient photopolymerization reactions than Runs 3.

CONCLUSIONS

In this article, the efficiency of the two and three-component PIS based on Py/amine/triazine to induce visible light polymerization of acrylates was studied. Triazine A was found more effective than EDB to start polymerization. However, the three-component system showed the best performance. Laser spectroscopy studies allowed the understanding of the processes that may explain the behavior observed in terms of photopolymerization. Py dyes react mainly through a singlet electron transfer mechanism from the dye to the triazine and from the amine to the dye. Beneficial side-reactions were shown to limit the photobleaching of the dye, resulting in highest final conversion. The effect of the relative concentration of the different additives on the whole efficiency of the process was also pointed out. A more detailed discussion will deserve a future work.

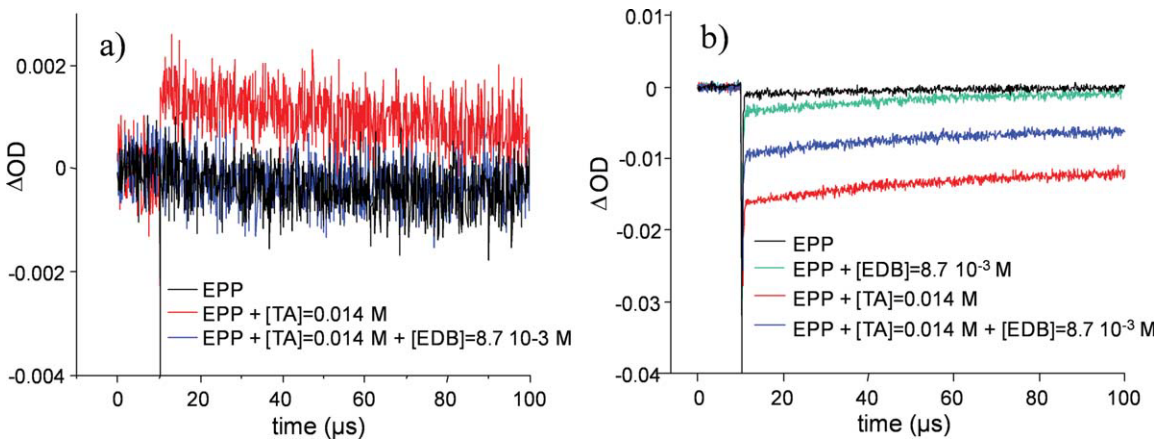

FIGURE 6 Kinetic traces recorded at (a) 400 nm and (b) 520 nm of an argon saturated solution of EPP alone and with the addition of TA and EDB.

The authors thank Dr. Suzuki and Prof. Takahara from the Chiba University for the synthesis of pyrromethene dyes.

REFERENCES AND NOTES

1 (a) Fouassier, J. P. In Photoinitiation, Photopolymerization, Photocuring; Hanser: Münich, 1995; (b) Photoinitiated Polymerization; Belfied, K. D.; Crivello, J. V., Eds.; ACS Symposium Series 847, American Chem Society: Washington, DC, 2003; (c) Schnabel, W. Polymers and Light: Fundamentals and Technical Applications; Wiley-VCH: Weinheim, D, 2007; (d) Basics and Applications of Photopolymerization Reactions; Fouassier, J. P.; Allonas, X., Eds., Research Signpost: Trivandrum, India, in press; (e) Davidson, S. In Exploring the Science, Technology and Application of UV and EB Curing; Sita Technology Ltd.: London, 1999; (f) Allonas, X.; Croutxe-Barghorn, C.; Fouassier, J. P.; Lalevée, J.; Malval, J. P.; Morlet-Savary, F. In Lasers in Chemistry, Vol. 2. Influencing Matter; Lackner, M., Ed.; Wiley, 2008; Chapter 35.

2 Roffey, C. In Photogeneration of Reactive Species for UV Curing; Wiley: Chichester, 1997.

3 Oster, G.; Yang, N. L. Chem Rev 1968, 68, 125–151.

4 Monroe, B. M.; Weed, G. C. Chem Rev 1993, 93, 435–448.

5 Encinas, M. V.; Rufs, A. M.; Bertolotti, S.; Previtali, C. M. Macromolecules 2001, 34, 2845–2847.

6 (a) Fouassier, J. P.; Ruhlmann, D.; Graff, B.; Takimoto, Y.; Kawabata, M.; Harada, M. J. Im Sci Techn 1993, 37, 208–210; (b) Fouassier, J-P; Erddalane, A; Morlet-Savary, F; Sumiyoshi, I; Harada, M; Kawabata, M. Macromolecules 1994, 27, 3349–3356; (c) Fouassier, J. P.; Morlet-Savary, F.; Yamashita, K.; Imahashi, S. Polymer 1997, 38, 1415–1421; (d) Allonas, X; Fouassier, J. P.; Kaji, M.; Miyasaka, M.; Hidaka, T. Polymer 2001, 42, 7627–7634; (e) Fouassier, J. P.; Chesneau, E. Makromol Chem 1991, 192, 1307–1315; (f) Grotzinger, C.; Burget, D.; Jacques, P.; Fouassier, J. P. Polymer 2003, 44, 3671–3677; (g) Fouassier, J. P.; Allonas, X.; Lalevée, J.; Visconti, M. J Polym Sci Part A: Polym Chem 2000, 38, 4531–4541; (h) Allonas, X.; Fouassier, J. P.; Kaji, M.; Murakami, Y. Photochem Photobiol Sci 2003, 2, 224–229.

7 (a) Cavitt, T. B.; Hoyle, C. E.; Kalyanaraman, V.; Jönsson, S. Polymer 2004, 45, 1119–1123; (b) Nguyen, C. K.; Hoyle, C. E.; Lee, T. Y.; Joensson, S. Eur Pol J 2007, 43, 172–177.

8 (a) Urano, T.; Hino, E.; Ito, H.; Shimizu, M.; Yamaoka, T. Polym Adv Technol 1998, 9, 825–830; (b) Urano, T.; Ito, H.; Yamaoka, T. Polym Adv Technol 1999, 10, 321–328.

9 Jockusch, S.; Timpe, H.-J.; Schnabel, W.; Turro, N. J. J Phys Chem 1997, 101, 440–445.

10 (a) Bi, Y.; Neckers, D. C. J. Photochem Photobiol A Chem 1993, 74, 221–230; (b) Bi, Y; Neckers, D. C. Macromolecules 1994, 27, 3683–3693.

11 Kabatc, J.; Zasada, M.; Paczkowski, J. J Polym Sci A: Polym Chem 2007, 45, 3626–3636.

12 Padon, K. S.; Scranton, A. B. J Polym Sci Part A: Polym Chem 2000, 38, 2057–2066.

13 (a) Kim, D.; Stansbury, J. W. J Polym Sci Part A: Polym Chem 2009, 47, 887–898; (b) Kim, D. K.; Stansbury, J. W. J Polym Sci Part A: Polym Chem 2009, 47, 3131–3141.

14 Eaton, D. F. Top Cur Chem 1990, 156, 199–225.

15 Boyer, J. H.; Haag, A. M.; Sathyamoorthi, G.; Soong, M. L.; Thangaraj, K.; Pavlopoulos, T. G. Heteroatom Chem 1993, 4, 39–49.

16 Pavlopoulos, T. G.; Boyer, J. H.; Shah, M.; Thangaraj, K.; Soong, M. L. Appl Opt 1990, 29, 3885–3886.

17 Karolin, J.; Johansson, L. B. A.; Strandberg, L.; Ny, T. J Am Chem Soc 1994, 116, 7801–7806.

18 Toele, P.; Zhang, H.; Trieflinger, C.; Daub, J.; Glasbeek, M. Chem Phys Lett 2003, 368, 66–75.

19 O'Neil, M. P. Opt Lett 1993, 18, 37–38.

20 Costela, A.; Garcia-Moreno, I.; Gomez, C.; Sastre, R.; Amat-Guerri, F.; Liras, M.; Lopez Arbeloa, F.; Banuelos Prieto, J.; Lopez Arbeloa, I. J Phys Chem A 2002, 106, 7736–7742.

21 Jones, G.; Kumar, S.; Klueva, O.; Pacheco, D. J Phys Chem A 2003, 107, 8429–8434.

22 Bergmann, A.; Holzer, W.; Stark, R.; Gratz, H.; Penzkofer, A.; Amat-Guerri, F.; Costela, A.; Garcia-Moreno, I.; Sastre, R. Chem Phys 2001, 271, 201–213.

23 Mula, S.; Ray, A. K.; Banerjee, M.; Chaudhuri, T.; Dasgupta, K.; Chattopadhyay, S. J Org Chem 2008, 73, 2146–2154.

24 García-Moreno, I.; Costela, A.; Campo, L.; Sastre, R.; Amat-Guerri, F.; Liras, M.; Arbeloa, F. L.; Prieto, J. B.; Arbeloa, I. L. J Phys Chem A 2004, 108, 3315–3323.

25 Blaya, S.; Acebal, P.; Carretero, L.; Fimia, A. Opt Com 2003, 228, 55–61.

26 Garcia, O.; Costela, A.; Garcia-Moreno, I.; Sastre, R. Macromol Chem Phys 2003, 204, 2233–2239.

27 Noppakundilograt, S.; Suzuki, S.; Urano, T.; Miyagawa, N.; Takahara, S.; Yamaoka, T. Polym Adv Technol 2002, 13, 527–533.

28 Suzuki, S.; Allonas, X.; Fouassier, J. P.; Urano, T.; Takahara, S.; Yamaoka, T. J. Photochem Photobiol A: Chem 2006, 181, 60–66.

29 Suzuki, S.; Allonas, X.; Fouassier, J. P.; Urano, T.; Takahara, S.; Yamaoka, T. In Photochemistry and UV Curing: New Trends; Fouassier, J. P., Ed; Research Signpost: Trivandrum, 2006; Chapter 38, pp 467–475.

30 Kawamura, K.; Kato, K. Polym Adv Technol 2004, 15, 324–328.

31 Grotzinger, C.; Burget, D.; Jacques, P.; Fouassier, J. P. Polymer 2003, 44, 3671–3677.

32 Mauguiere-Guyonnet, F.; Burget, D.; Fouassier, J. P. Prog Org Coating 2007, 59, 37–45.

33 Grotzinger, C.; Burget, D.; Jacques, P.; Fouassier, J. P. Macromol Chem Phys 2001, 202, 3513–3522.

34 Shah, M.; Thangaraj, K.; Soong, M. L.; Wolford, L. T.; Boyer, J. H.; Politzer, I. R.; Pavlopoulos, T. G. Heteroatom Chem 1990, 1, 389–399.

35 Sathyamoorthi, G.; Boyer, J. H.; Allik, T. H.; Chandra, S. Heteroatom Chem 1994, 5, 403–407.

36 Decker, C.; Moussa, K. Macromolecules 1989, 22, 4455–4462.

37 Allonas, X.; Fouassier, J. P.; Angiolini, L.; Caretti, D. Helv Chim Acta 2001, 84, 2577–2588.

38 Dossot, M.; Allonas, X.; Jacques, P. J Photochem Photobiol A: Chem 1999, 128, 47–55.

39 Dossot, M.; Allonas, X.; Jacques, P. Res Chem Interm 2003, 29, 21–34.

40 Rehm, D.; Weller, A. Isr J Chem 1970, 8, 259.

41 Pohlers, G.; Scaiano, J. C.; Sinta, R.; Brainard, R.; Pai, D. Chem Mater 1997, 9, 1353–1361.

42 Li, F.; Ciringh, Y.; Seth, J.; Martin, C. H.; Singh, D. L.; Kim, D.; Birge, R. R.; Bocian, D. F.; Holten, D. J Am Chem Soc 1998, 120, 10001–10017.

43 López Arbeloa, F.; López Arbeloa, T.; López Arbeloa, I. J Photochem Photobiol A: Chem 1999, 121, 177–182.

44 Arbeloa, T. L.; Arbeloa, F. L.; Arbeloa, I. L.; Garcia-Moreno, I.; Costela, A.; Sastre, R.; Amat-Guerri, F. Chem Phys Lett 1999, 299, 315–321.